Energy emission from a high curvature region and its backreaction

Takafumi Kokubu,[1,4,*] Sanjay Jhingan,[2,3,†] and Tomohiro Harada[4,‡]

[1]*Theory Center, Institute of Particle and Nuclear Studies, High Energy Accelerator Research Organization (KEK), Tsukuba, 305-0801, Japan*
[2]*iCLA, Yamanashi Gakuin University, Kofu, Yamanashi, 400-8575, Japan*
[3]*Centre for Theoretical Physics, Jamia Millia Islamia, New Delhi, 110025, India*
[4]*Department of Physics, Rikkyo University, Toshima, Tokyo, 171-8501, Japan*

(Received 16 February 2018; published 14 May 2018)

A strong gravity naked singular region can give important clues toward understanding the classical as well as spontaneous nature of General Relativity. We propose here a model for energy emission from a naked singular region in a self-similar dust spacetime by gluing two self-similar dust solutions at the Cauchy horizon. The energy is defined and evaluated as a surface energy of a null hypersurface, the null shell. Also included are scenarios of the spontaneous creation or disappearance of a singularity, the end of inflation, black hole formation, and bubble nucleation. Our examples investigated here explicitly show that one can model unlimitedly luminous and energetic objects in the framework of General Relativity.

DOI: 10.1103/PhysRevD.97.104014

I. INTRODUCTION

The recent discoveries of gravitational waves [1–5] have provided us with the opportunity to study strong gravitational field environments created by coalescing binary black holes and neutron stars. Having established General Relativity (GR) as the classical theory in the strong gravity regime, these discoveries have also opened new exciting areas of research such as gravitational wave astronomy and multimessenger astronomy [6]. However, theoretically, GR predicts that under quite generic initial conditions continued gravitational collapse should end in a singularity, i.e., regions of arbitrarily high spacetime curvature [7–9]. Thus, black holes as a unique end state of continued gravitational collapse are contingent on an additional requirement of the cosmic censorship conjecture (CCC) [10]. The essence of this conjecture is that the singularity should always be safely hidden behind a horizon. This can be achieved by the formation of trapped surfaces that form during collapse and surround the singularity, hiding it from the outside world. One could, perhaps, also argue that before the mathematical structure of spacetime breaks down some quantum gravity effects, due to the breakdown of classical theory, should prevent singularity formation. However, with no viable quantum theory for gravity in sight, the physics of such dense regions in spacetime remains an open question. Interestingly, GR all by itself does not say anything about the causal nature of these singularities. Therefore, agreement between GR and strong gravity observations has also renewed interest in the formation of naked singularities as an additional possibility of the end state of gravitational collapse.

The study by Oppenheimer and Snyder (OS) provides a paradigm for black hole formation in continued gravitational collapse [11]. This simple model of a spherically symmetric homogeneous dust ball (perfect fluid with no pressure) elegantly captures salient features characterizing a black hole, namely, the formation of a central singularity, an apparent horizon, and an event horizon. The OS model led to the establishment viewpoint that end state of continued gravitational collapse leads to the formation of a black hole (CCC). Numerous counterexamples to the CCC have also appeared in the studies generalizing the OS model, i.e., the formation of a singularity that can be seen by an external observer. Such a naked singularity can form an end state of a collapsing inhomogeneous dust cloud [12–16]. There are radial null geodesics starting from the singularity. With an appropriate choice of initial data, null geodesics can reach the null infinity, and thus the singularity can be globally naked.

The counterexamples to the censorship hypothesis are not limited to dust only. Gravitational collapse in matter models with pressure are investigated as well. The spherically symmetric self-similar spacetime filled with a perfect fluid forms a naked singularity if an equation of state is soft enough [14]. Furthermore, naked singularity also forms when the assumption of self-similarity is relaxed [17,18] (see also Ref. [19]). The generalization of geometry to quasispherical or cylindrical also does not help restore

*kokubu@post.kek.jp, 14ra002a@rikkyo.ac.jp
†sanjay.jhingan@gmail.com
‡harada@rikkyo.ac.jp

 © 2018 American Physical Society

the CCC [20]. Thus, the studies so far indicate that arbitrarily high curvature regions, akin to a naked singularity, can form during the collapse.

The extreme curvature region around the singularity is expected to give rise to high-energy phenomena. Since there is virtually no upper limit to energy that can be achieved due to strong curvatures, highly energetic phenomena in the Universe, such as a gamma-ray burst, can be from a region around a strong curvature naked singularity. However, these studies are speculative in nature, and it is a challenge to create a concrete model that can serve to explain the origin of high-energy phenomena like a gamma-ray burst. There are few qualitative [21,22] and quantitative studies [23–34] in this direction. Classical gravitational radiation of spacetimes filled with dust matter was studied in Refs. [35–37].

As mentioned above, a self-similar dust universe with an appropriate initial matter distribution forms a naked singularity. The fastest of these geodesics from the singular center defines the Cauchy horizon. In a spherically symmetric spacetime geometry, starting from the singular center, the Cauchy horizon expands radially, and the region beyond the horizon is by definition undetermined. Since the Cauchy horizon is a null hypersurface, we use the null version of junction conditions to replace the inside of the Cauchy horizon by another well-behaved spacetime, removing singularity and restoring predictability.

The aim of this paper is to propose various models for physical processes such as energy emission from singular regions, the spontaneous creation of a singularity, negative-mass black holes, the decay of Minkowski spacetime, a scenario for the end of inflation, and the spontaneous creation of black holes, using matching across two null hypersurfaces. The matching across two null hypersurfaces was pioneered by Israel and collaborators (see Ref. [38] and references therein). To achieve our goal, we use dust models that are known to harbor nakedly singular solutions.

The paper is organized as follows. In Sec. II, we give a brief overview of null-shell formalism describing an expanding or contracting null surface that partitions a spacetime into two parts. Section III contains several examples based on the general formalism. We conclude with Sec. IV. Units $c = G = 1$ are adopted throughout this paper.

II. SPHERICALLY SYMMETRIC NULL SHELL: GENERAL FORMALISM

We give a quick overview of the general formalism that describes an expanding or imploding null hypersurface with a finite surface energy and pressure in spherically symmetric spacetimes. Whereas the spherically symmetric case is discussed in Ref. [39], the analysis and notation used here are in view of the examples discussed later in the paper. The formalism models the energy and the pressure as the quantities defined on the boundary of two matched spacetimes. The goal here is to calculate the energy that such a null surface (Σ) would have. The spacetime metrics on either side of Σ are given by

$$\mathrm{d}s_{\pm}^2 = A_{\pm}(t_{\pm}, r_{\pm})\mathrm{d}t_{\pm}^2 + B_{\pm}(t_{\pm}, r_{\pm})\mathrm{d}r_{\pm}^2 + C_{\pm}(t_{\pm}, r_{\pm})(\mathrm{d}\theta^2 + \sin^2\mathrm{d}\varphi^2). \tag{1}$$

Here, $4\pi C(t, r)$ is equivalent to the physical surface area of a sphere at coordinates t and r. We identify spacetimes on the either side of null hypersurface (Σ) by $+$ and $-$ signs.

For completeness, we give here the nonzero Christoffel symbols for the metric above (the $\pm$ sign is omitted),

$$\Gamma^t_{tt} = \frac{\dot{A}}{2A}, \quad \Gamma^t_{tr} = \frac{A'}{2A}, \quad \Gamma^t_{rr} = -\frac{\dot{B}}{2A}, \quad \Gamma^t_{\theta\theta} = -\frac{\dot{C}}{2A},$$
$$\Gamma^t_{\varphi\varphi} = -\frac{\dot{C}}{2A}\sin^2\theta, \quad \Gamma^r_{rr} = \frac{B'}{2B}, \quad \Gamma^r_{tr} = \frac{\dot{B}}{2B}, \quad \Gamma^r_{tt} = -\frac{A'}{2B},$$
$$\Gamma^r_{\theta\theta} = -\frac{C'}{2B}, \quad \Gamma^r_{\varphi\varphi} = -\frac{C'}{2B}\sin^2\theta, \quad \Gamma^\theta_{t\theta} = \frac{\dot{C}}{2C}, \quad \Gamma^\theta_{r\theta} = \frac{C'}{2C},$$
$$\Gamma^\theta_{\varphi\varphi} = -\sin\theta\cos\theta, \quad \Gamma^\varphi_{t\varphi} = \frac{\dot{C}}{2C}, \quad \Gamma^\varphi_{r\varphi} = \frac{C'}{2C}, \quad \Gamma^\varphi_{\theta\varphi} = \cot\theta, \tag{2}$$

where $\cdot \coloneqq \partial/\partial t$ and $' \coloneqq \partial/\partial r$.

A. Null hypersurface Σ

As we are interested in emission (absorption) from a naked singularity, the two spacetimes are matched along expanding (imploding) null surfaces. The equation describing such a surface is given by the outgoing (incoming) radial null geodesics in $\mathcal{M}^{\pm}$, i.e.,

$$\frac{\mathrm{d}t_{\pm}}{\mathrm{d}r_{\pm}} = \epsilon_{\pm}\sqrt{\frac{B_{\pm}}{|A_{\pm}|}}. \tag{3}$$

Note that $A = -|A|$ for outside of the horizon (if any), and $\epsilon_{\pm}$ is defined by

$$\epsilon_+ \coloneqq \begin{cases} +1 & :\text{outgoing} \\ -1 & :\text{incoming} \end{cases}, \qquad \epsilon_- \coloneqq \begin{cases} +1 & :\text{outgoing} \\ -1 & :\text{incoming} \end{cases}. \tag{4}$$

The sign of ϵ represents null rays to be outgoing or incoming. One can choose a specific null geodesic in $\mathcal{M}^{\pm}$, which characterizes null hypersurfaces Σ_+ and Σ_- in $\mathcal{M}^+$ and $\mathcal{M}^-$, respectively. The hypersurfaces Σ_+ and Σ_- are identified so that the two spacetimes are glued along these null hypersurfaces, i.e., $\Sigma_+ = \Sigma_- \eqqcolon \Sigma$. In this sense, the null hypersurface Σ partitions the spacetime into two regions: the past ($\mathcal{M}^-$) and the future ($\mathcal{M}^+$) of Σ (Fig. 1).

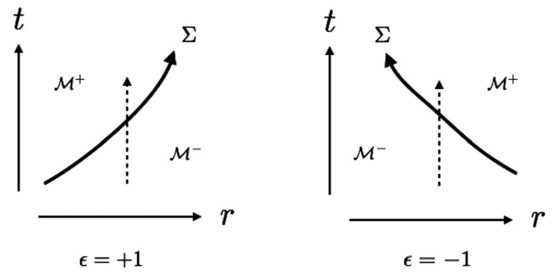

FIG. 1. Schematic figure for null matching. Null hypersurface Σ partitions a spacetime into two regions, past ($\mathcal{M}^-$) and future ($\mathcal{M}^+$), of Σ. The dashed line is the world line of an observer at fixed spatial coordinates.

The two metrics must be the same on Σ, i.e., $\mathrm{d}s_+^2|_\Sigma = \mathrm{d}s_-^2|_\Sigma$, and from Eq. (1), the coefficient of the angular part gives a relation between C_+ and C_-:

$$C_+(t_+(r_+), r_+)|_\Sigma = C_-(t_-(r_-), r_-)|_\Sigma. \tag{5}$$

B. Null hypersurface: Intrinsic coordinates

To implement the null-shell formalism, we first consider a system of coordinates intrinsic to the hypersurface Σ,

$$y^l = (\lambda, \theta, \varphi);$$

here, λ is an arbitrary parameter characterizing generators on the null hypersurface. The hypersurface can be described as $x_\pm^\alpha = (t_\pm(\lambda), r_\pm(\lambda), \theta, \varphi)$ in terms of coordinates on either side. Thus, the parametric equations for the null hypersurface Σ, as seen from either side, are

$$t_\pm = t_\pm(r_\pm(\lambda)), \qquad r_\pm = r_\pm(\lambda), \qquad \theta = \theta, \qquad \varphi = \varphi. \tag{6}$$

The vectors k^α, tangent to the null hypersurface on each side, are given by

$$k_\pm^\alpha \partial_\alpha = \left.\frac{\mathrm{d}t_\pm}{\mathrm{d}r_\pm}\right|_\Sigma \overset{\circ}{r}_\pm \partial_t + \overset{\circ}{r}_\pm \partial_r, \tag{7}$$

where $\circ := \mathrm{d}/\mathrm{d}\lambda$. Because a radial null geodesic equation for Σ is given by Eq. (3), $k_\pm^\alpha$ reduces to

$$k_\pm^\alpha \partial_\alpha = \epsilon_\pm \sqrt{\frac{B_\pm}{|A_\pm|}} \overset{\circ}{r}_\pm \partial_t + \overset{\circ}{r}_\pm \partial_r. \tag{8}$$

Vector fields $e_{(\theta)}^\alpha \partial_\alpha = \partial_\theta$ and $e_{(\varphi)}^\alpha \partial_\alpha = \partial_\varphi$ are also tangent to Σ. Moreover, auxiliary null vector fields $N_\pm^\alpha$ satisfying $N_\pm^\alpha k_{\alpha\pm} = -1$, $N_\pm^\alpha N_{\alpha\pm} = 0$, and $N_\pm^\alpha e_{\alpha\pm} = 0$ are obtained as

$$N_\alpha^\pm \mathrm{d}x^\alpha = -\frac{\epsilon_\pm}{2\overset{\circ}{r}_\pm} \sqrt{\frac{|A_\pm|}{B_\pm}} \mathrm{d}t - \frac{1}{2\overset{\circ}{r}_\pm} \mathrm{d}r. \tag{9}$$

Vectors k^α, $e_{(\theta)}^\alpha$, $e_{(\varphi)}^\alpha$, and N^α complete a basis on Σ [39].

C. Surface stress-energy tensor and transverse curvature

We calculate the surface stress-energy tensor, i.e., a stress-energy tensor on Σ, which is written as

$$T_\Sigma^{\alpha\beta} = (-k^\gamma u_\gamma)^{-1} S^{\alpha\beta} \delta(\tau), \tag{10}$$

where

$$S^{\alpha\beta} := \mu k^\alpha k^\beta + p \sigma^{AB} e_{(A)}^\alpha e_{(B)}^\beta.$$

Here, μ and p are interpreted as the surface energy density and the surface pressure on the null hypersurface, respectively. The parameter τ was introduced as the proper time of an observer who has the 4-velocity u^α; it takes a zero value while crossing Σ. Defining transverse curvature C_{lm} as

$$C_{lm} := -N_\alpha e_{(l);\beta}^\alpha e_{(m)}^\beta,$$

we can write the explicit expressions for the energy density μ and the pressure p as

$$8\pi\mu := -\sigma^{ab}[C_{ab}], \qquad 8\pi p := -[C_{\lambda\lambda}]. \tag{11}$$

The indices l and m run through λ, θ, and φ, and a and b run through θ and ϕ. The standard notation $[A] := A_+|_\Sigma - A_-|_\Sigma$ is used for measuring the jump in scalar qualities at Σ.

The general expressions for the nonzero components of transverse curvature can be calculated as (hereafter, the $\pm$ sign is omitted for clarity)

$$C_{\lambda\lambda} = \overset{\circ}{r} \left\{ \epsilon \frac{\dot{B}}{\sqrt{|A|B}} + \frac{1}{2}(\ln|A|)' + \frac{1}{2}(\ln B)' \right\}, \tag{12}$$

$$C_{ab} = -\frac{\sigma_{ab}}{4C\overset{\circ}{r}} \left(-\frac{\epsilon \dot{C}}{\sqrt{|A|B}} + \frac{C'}{B} \right), \tag{13}$$

where $\sigma_{ab} \mathrm{d}x^a \mathrm{d}x^b := C(\mathrm{d}\theta^2 + \sin^2\theta \mathrm{d}\varphi^2)$.

D. Parameter-independent description for the shell's whole energy and relation to its luminosity

We define the integrated energy over a spherical shell, which would be measured by an observer who is in $\mathcal{M}^-$ with a 4-velocity u_α^-, as

$$E_{\mathrm{shell}} := 4\pi C T_{\alpha\beta} u_-^\alpha u_-^\beta|_\Sigma. \tag{14}$$

We should note that the quantity E_{shell} is actually related to a *luminosity* emitted from the system. Luminosity of the shell can be defined as the area integration of energy flux that would be measured by a comoving observer at infinity (which means he/she is a static observer), who has the 4-velocity u^α. In equation form, this is written as

$$L_{\mathrm{shell}} := 4\pi C T_{\alpha\beta} u^\alpha n^\beta|_\Sigma, \tag{15}$$

where n^β is one of three spacelike unit basis vectors that are orthogonal to u^α and its component toward to the direction in which the shell moves:

$$n^\alpha \partial_\alpha = \partial_r, \qquad n^\alpha n_\alpha = 1, \qquad u^\alpha n_\alpha = 0. \tag{16}$$

By geometrical observation, one identifies the null vector k^α is proportional to $u^\alpha + n^\alpha$: $k^\alpha = b(u^\alpha + n^\alpha)$ with $b =$ constant. Using all properties for k^α, u^α, and n^α, $E_{\rm shell}$ and $L_{\rm shell}$ reduce to

$$E_{\rm shell} = 4\pi C(-b)\mu, \tag{17}$$

$$L_{\rm shell} = 4\pi C(-b)\mu. \tag{18}$$

Thus, we have the relation

$$E_{\rm shell} = L_{\rm shell}. \tag{19}$$

$E_{\rm shell}$ (or equivalently $L_{\rm shell}$) is derived by junction conditions, and thus this is a function of the both of the metrics, $g^+_{\mu\nu}$ and $g^-_{\mu\nu}$. However, since we observe $E_{\rm shell}$ from the either side of the two spacetimes, the final description of physical quantities $E_{\rm shell}$ must be written in the metric in the one side. The two metrics are related each other through Eq. (5). We will denote $E_{\rm shell}$ by the metric on the $-$ side. To do so, consider Eq. (5); it relates r_+ and r_-, say,

$$r_+ = \psi(r_-). \tag{20}$$

The explicit functional form of ψ can be determined once the line elements $\mathcal{M}^+$ and $\mathcal{M}^-$ are fixed. Since $r_\pm$ is parametrized by λ, differentiation of Eq. (20) gives

$$\mathring{r}_+ = \frac{d\psi(r_-)}{dr_-}\mathring{r}_-. \tag{21}$$

Using Eqs. (20) and (21), we can eliminate r_+ and $\mathring{r}_+$ from the expressions of μ and p. Consequently, the energy $E_{\rm shell}$ becomes a function of r_- only.

III. EXAMPLES

A. Energy emission from a naked singularity: Self-similar dust collapse

We consider naked singularity formation in self-similar dust collapse. We consider two spacetime manifolds $\mathcal{M}^+$ and $\mathcal{M}^-$ as two spherically symmetric dust spacetimes of which the metrics are given by

$$ds^2_\pm = -dt^2_\pm + (R'_\pm)^2 dr^2_\pm + R^2_\pm (d\theta^2 + \sin^2\theta d\varphi^2), \tag{22}$$

where $R_\pm = R_\pm(t_\pm, r_\pm)$. Or equivalently, from Eq. (1), we adopt the functions as follows:

$$A_\pm = -1, \qquad B_\pm = (R'_\pm)^2, \qquad C_\pm = R^2_\pm, \qquad \epsilon_\pm = 1. \tag{23}$$

Th stress-energy tensor for dust is given by $T^{\alpha\beta}_\pm = \rho_\pm(t,r) u^\alpha_\pm u^\beta_\pm$, with the comoving 4-velocity of dust $u^\alpha_\pm = \delta^\alpha_0$ and dust energy density $\rho_\pm(t,r)$. The nontrivial Einstein field equations derived from the above metric and stress-energy tensor yield (the $\pm$ sign is omitted for brevity)

$$\dot{R}^2 = \frac{F(r)}{R}, \tag{24}$$

$$F' = 8\pi\rho R^2 R', \tag{25}$$

where $F(r)$ is an arbitrary function of r. Using the remaining scaling freedom, we set $R(0,r) =: r$, and Eq. (25) can now be integrated to fix F in terms of the initial density profile $\rho(0,r)$ as

$$F(r) = 8\pi \int \rho(0,r) r^2 dr. \tag{26}$$

Hence, F is twice the mass interior of a sphere of radius r.

Equations (24) and (25) can be solved simultaneously for the unknown metric function R,

$$R^{3/2} = r^{3/2} - \frac{3}{2}\sqrt{F}t. \tag{27}$$

This solution is known as the marginally bound Lemaître-Tolman-Bondi (LTB) solution. If one takes the linear mass function, i.e., $F = 2\kappa r$, we have (with recovering the $\pm$ sign)

$$R^{3/2}_\pm = r^{3/2}_\pm \left(1 - a_\pm \frac{t_\pm}{r_\pm}\right), \tag{28}$$

where $a_\pm := 3\sqrt{2\kappa_\pm}/2$ and $\kappa_\pm$ is assumed to be a non-negative constant. Minkowski spacetime is recovered for $\kappa_\pm = 0$. We also note here that the spacetime of Eq. (22) with the metric function of the form Eq. (28) admits self-similarity [40]. To maintain simplicity and clarity in further discussion, the attention is restricted to the self-similar solution. However, with some difficulty, the discussion can be extended to the non-self-similar case also.

In this well-studied setup, the singularity forms first at the symmetry center $(t,r) = (0,0)$, and this can be globally naked for a range of values of parameter κ, characterizing the strength of gravity [41]. The actual value of the parameter range is not important, and from now on, the discussion assumes spacetime with the presence of a naked singularity. Considering radial null geodesics emanating from the singularity at the center, the Cauchy horizon is defined as the fastest null ray coming out of the singularity. To identify the equation of the Cauchy horizon, we first identify the family of singular outgoing radial null geodesics. From Eq. (22), the outgoing radial null geodesics obey the equation $dt/dr = R'$ (we omit the $\pm$ sign from expressions for brevity), which is explicitly written as

$$\frac{\mathrm{d}t}{\mathrm{d}r} = \frac{3r - at}{3r^{2/3}(r - at)^{1/3}}. \tag{29}$$

The condition for the existence of outgoing radial null rays, meeting central singularity $(t, r) = (0, 0)$ in their past with a positive finite slope, can be reduced to a finite nonzero positive value of the limit

$$\lim_{t\to 0, r\to 0} \frac{t}{r} = \lim_{t\to 0, r\to 0} \frac{\mathrm{d}t}{\mathrm{d}r} = z, \tag{30}$$

where z takes a constant value. The first equality in the equation above holds due to l'Hôpital's rule. Then, Eq. (29) reduces to a quartic equation (restoring the $\pm$ sign):

$$f(z_\pm) \coloneqq a_\pm z_\pm^4 - \left(1 + \frac{a_\pm^3}{27}\right) z_\pm^3 + \frac{a_\pm^2}{3} z_\pm^2 - a_\pm z_\pm + 1 = 0. \tag{31}$$

Using properties of quartic equations, in Eq. (31), some information on the nature of roots can be determined from discriminant $D = (-4a_\pm^6 + 2808a_\pm^3 - 729)/27$. If $D < 0$, the quartic has two real roots, and for $D = 0$, there is one real root. D is negative when $0 \leq a_\pm < a_* \coloneqq 3/(2(26 + 15\sqrt{3}))^{1/3} = 0.638014$ and vanishes when $a_\pm = a_*$.[1] The range of $a_\pm$ implies $0 \leq \kappa_\pm \leq \kappa_* \coloneqq 0.0904583$. In the self-similar dust solution, Eqs. (22) and (28), the Cauchy horizon takes the form

$$t_\pm = z_{ch}^\pm r_\pm, \tag{32}$$

where z_{ch}^+ and z_{ch}^- are the positive constants in $\mathcal{M}^+$ and $\mathcal{M}^-$, respectively. These are the smallest positive values of the solution to Eq. (31).

We consider matching two self-similar dust spacetimes at their Cauchy horizons, which are given by Eq. (32). So, the Cauchy surface is that null hypersurface Σ that partitions the spacetime into two regions: the past and the future of Σ. The matching procedure imposes restrictions on the metric function and its first derivative, respectively, the first and the second fundamental forms.

We start with the identification of outgoing null geodesics in two spacetimes. Recall, from Eq. (22), the outgoing radial null geodesics are

$$\frac{\mathrm{d}t_\pm}{\mathrm{d}r_\pm} = R'_\pm. \tag{33}$$

The matching of the first fundamental form, equivalent to condition (5), implies that metrics are the same on Σ, yielding $R_+|_\Sigma = R_-|_\Sigma$, i.e.,

$$(1 - a_+ z_{ch}^+)^{2/3} r_+|_\Sigma = (1 - a_- z_{ch}^-)^{2/3} r_-|_\Sigma. \tag{34}$$

Here, we have used the equation $t_\pm/r_\pm = z_{ch}^\pm$ on Σ. Equation (34) is our first fundamental form, and this gives a relation between r_+ and r_- on Σ.

The null hypersurface in parametric form can be written as

$$t_\pm = z_{ch}^\pm r_\pm(\lambda), \qquad r_\pm = r_\pm(\lambda), \qquad \theta = \theta, \qquad \varphi = \varphi. \tag{35}$$

We now construct the explicit set of basis vectors for the self-similar case under consideration to implement the null-shell formalism. From Eq. (8), the tangent null vector $k_\pm^\alpha$ is given by

$$k_\pm^\alpha \partial_\alpha = z_{ch}^\pm \mathring{r}_\pm \partial_t + \mathring{r}_\pm \partial_r. \tag{36}$$

The spatial unit tangents to a sphere are given by $e^{\alpha\pm}_{(\theta)}\partial_\alpha = \partial_\theta$ and $e^{\alpha\pm}_{(\varphi)}\partial_\alpha = \partial_\varphi$. The auxiliary null vector $N_\pm^\alpha$ is written by Eq. (9) as

$$N_\pm^\alpha \partial_\alpha = -\frac{1}{2z_{ch}^\pm \mathring{r}_\pm}\partial_t - \frac{1}{2(z_{ch}^\pm)^2 \mathring{r}_\pm}\partial_r. \tag{37}$$

Now that we have explicit expressions for the basis vectors above, we have the tools to implement the junction conditions for matching two null hypersurfaces. The nonzero components of the transverse curvature, Eqs. (12) and (13), are

$$C_{\lambda\lambda}^\pm = \mathring{r}_\pm \frac{2a_\pm^2 z_{ch}^\pm}{9r_\pm(1 - a_\pm z_{ch}^\pm)^{4/3}}, \tag{38}$$

$$C_{ab}^\pm = -\frac{1}{\mathring{r}_\pm}\frac{\sigma_{ab}}{2z_{ch}^\pm R_\Sigma^\pm}\left(\frac{2a_\pm}{3(1 - a_\pm z_{ch}^\pm)^{1/3}} + 1\right), \tag{39}$$

where $\sigma_{ab}\mathrm{d}x^a\mathrm{d}x^b \coloneqq R^2(\mathrm{d}\theta^2 + \sin^2\theta\mathrm{d}\varphi^2)$.

Consequently, μ and p can be written as

$$8\pi\mu = \frac{1}{z_{ch}^+ R_\Sigma^+ \mathring{r}_+}\left(\frac{2a_+}{3(1 - a_+ z_{ch}^+)^{1/3}} + 1\right) - \frac{1}{z_{ch}^- R_\Sigma^- \mathring{r}_-}\left(\frac{2a_-}{3(1 - a_- z_{ch}^-)^{1/3}} + 1\right), \tag{40}$$

$$8\pi p = -\mathring{r}_+ \frac{2a_+^2 z_{ch}^+}{9r_+(1 - a_+ z_{ch}^+)^{4/3}} + \mathring{r}_- \frac{2a_-^2 z_{ch}^-}{9r_-(1 - a_- z_{ch}^-)^{4/3}}. \tag{41}$$

As can be seen from expressions (40) and (41), the surface energy and the surface pressure are determined by fixing

[1] In fact, the condition $D < 0$ gives two possible ranges for a, $0 \leq a < a_* = 0.638$ or $a > a_* = 8.886$. However, the larger range of a_* is unphysical because outgoing radial null geodesics form after the shell focusing singularity [42].

the initial data, namely, the parameter κ_+ and κ_-. The $\mathring{r}_+$, in the equations above, is related to $\mathring{r}_-$ through Eq. (34). Clearly, no surface energy and pressure are carried if $a_+ = a_-$ (or equivalently $\kappa_+ = \kappa_-$); i.e., the initial profile κ is the same in $\mathcal{M}^+$ and $\mathcal{M}^-$. If $a_- < a_+$, $E_{\rm shell} > 0$, and for $E_{\rm shell} < 0$, $a_- > a_+$.

From Eq. (14), the energy of the null shell $E_{\rm shell}$ that is measured by an observer in the past of Σ [we see Σ from the $(-)$ side] with the 4-velocity u^α_- is

$$E_{\rm shell} = 4\pi R^2 T^{\alpha\beta} u^-_\alpha u^-_\beta|_{\tau=0}. \tag{42}$$

For a comoving observer choosing the 4-velocity to be $u^\alpha_- \partial_\alpha = \partial_t$, the expression for energy (42) takes the form

$$E_{\rm shell} = 4\pi R^2_\Sigma(-k^\gamma_- u^-_\gamma)\mu. \tag{43}$$

One calculates $-k^\gamma_- u^-_\gamma = \mathring{r}_- R'_-$, and hence Eq. (43) reduces to

$$E_{\rm shell} = \frac{R_\Sigma}{2}\left\{\frac{(1-a_+ z^+_{ch})^{2/3} z^-_{ch}}{(1-a_- z^-_{ch})^{2/3} z^+_{ch}}\left(\frac{2a_+}{3}(1-a_+ z^+_{ch})^{-1/3}+1\right) - \left(\frac{2a_-}{3}(1-a_- z^-_{ch})^{-1/3}+1\right)\right\}. \tag{44}$$

One can see that $E_{\rm shell}$ is a linear function of R_Σ. The numerical plot for $E_{\rm shell}/R_\Sigma$ in Eq. (44) is shown in Fig. 2.

Figure 2 describes the variation of the ratio $E_{\rm shell}/R_\Sigma$ with a_+, the energy density parameter of the matched spacetime, for fixed values of a_-. The parameters, a_+ and a_-, take values in the following range: $0 \le a_+ \le a_- \le a_*$. For a fixed value of a_-, the ratio E/R decreases with the increase in a_+ and vanishes for $a_+ = a_-$ due to the positivity of energy emitted. The maximum emission for a given a_- lies at $a_+ = 0$, which corresponds to Minkowski spacetime in the matched region. Physically, this implies all the energy in M_- is emitted along the null shell. For the largest allowed value of $a_- = a_*$, beyond which M_- evolves into a black hole spacetime geometry, $E_{\rm shell}/R_\Sigma$ is the largest for $a_+ = 0$.

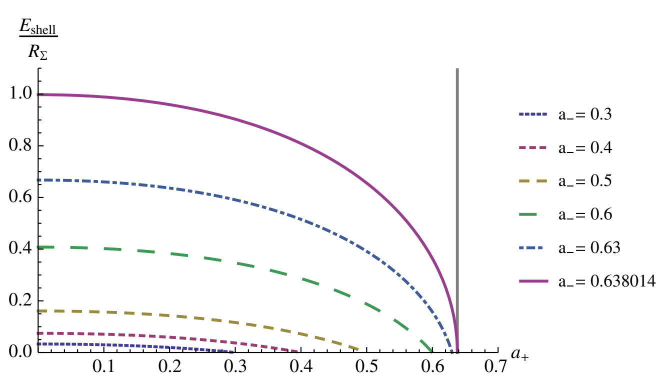

FIG. 2. $E_{\rm shell}/R_\Sigma$ versus a_+. The vertical solid line is at $a_+ = a_* = 0.638014$. $E_{\rm shell}/R_\Sigma$ is positive only for $0 \le a_+ < a_- \le a_*$. The more the gap between a_- and a_+ increases, the more $E_{\rm shell}/R_\Sigma$ is.

Both in the dust case (the model given in the present paper) and in the Vaidya case (Jhingan *et al.*'s model [44]), the surface energy μ is proportional to r^{-1}. This fact implies that the whole energy of the null shell, $E_{\rm shell}$, grows in proportion to r (or equivalently R_Σ) and hence diverges at spatial infinity. This blowup feature is essentially due to the self-similarity of spacetimes. The reason is the following: regardless of whether spacetime is self-similar or not, the surface energy μ has a dimension of $1/(\text{length})$. When we restrict our attention to self-similar spacetime, then the description of μ must be of the form $F(z)/r$, where $z \coloneqq t/r$. Because z is constant on the Cauchy horizon (and also on the event horizon) in the self-similar metric, F becomes $F(z_{ch})$, which is definitely constant. Thus, $E_{\rm shell} \propto 4\pi(R|_\Sigma)^2\mu$ [where $R|_\Sigma = r|_\Sigma(1-az_{ch})^{2/3}$ in our dust model and $R|_\Sigma = r|_\Sigma$ in the Vaidya model] must be proportional to r (or equivalently R_Σ) under the self-similar assumption.

We give a physical interpretation of the increasing energy of the null shell. Take the conservation law for the null shell, which is given by Poisson's book [39] as

$$p\frac{\mathrm{d}}{\mathrm{d}\lambda}\delta S + [T_{\alpha\beta}k^\alpha k^\beta]\delta S = 0, \tag{45}$$

where $\delta S \coloneqq C\sin^2\theta \mathrm{d}\theta\mathrm{d}\varphi$ is an element of cross sectional area on the shell. The first term on the left-hand side of Eq. (45) is the work done by the shell's expansion, while the second term is the energy absorbed into the shell from its surrounding. Physical interpretation for the growing of the shell energy $4\pi R^2\mu$ is that the null shell expands in an imploding dust region while absorbing the energy of the surrounding dust.

1. Instant singularity

For an interesting example of our model, one can consider an exclusive situation, say, "a singularity in an instant": a singularity disappears immediately after its occurrence. To describe this, let us take $0 < \kappa_- \le \kappa_*$ in the past of Σ. Then, a singularity forms in a finite time. In the $(+)$ side, we take $\kappa_+ = 0$ $(a_+ = 0)$, the minimum value of κ. Vanishing κ represents the Minkowski spacetime. Since $\mathcal{M}^+$ is defined as the future of Σ, the above setup describes an instant presence of a singularity. The singularity exists only at the point $(t,r) = (0,0)$. For $a = 0$, we have $z_{ch} = 1$ from Eq. (31). Thus, in this scenario, the energy of the shell that appeared from the point $(t,r) = (0,0)$ reduces to

$$E_{\rm shell} = \frac{R_\Sigma}{6}\left\{\frac{3z^-_{ch}}{(1-a_- z^-_{ch})^{2/3}} - (2a_-(1-a_- z^-_{ch})^{-1/3}+3)\right\}. \tag{46}$$

For simplicity, let us take $a_- = a_* \Leftrightarrow \kappa_- = \kappa_*$, the maximum value of κ. For $a = a_* = 0.638014$, z_{ch} is solved as $z_{ch}(a_*) = 1.25992$. By putting these values into Eq. (46), we have $E_{\rm shell} = R_\Sigma$.

According to this scenario, a region of the dust matter is pushed away from the center by the motion of outgoing null shell.

B. Energy emission from a naked singularity: Negative-mass Schwarzschild solution

We have considered an isotropic emission of radiation from a naked singularity by modeling two self-similar LTB spacetimes with different density profiles in the first example. Here, we consider another emission scenario that describes a null emission from a singularity after dust collapse in which the final singularity has negative mass. This situation is modeled by taking $\mathcal{M}^-$ as the LTB solution, while $\mathcal{M}^+$ is a negative-mass Schwarzschild solution,

$$A_- = -1, \qquad B_- = (R'(t_+, r_+))^2, \qquad C_- = R(t_+, r_+)^2,$$
$$A_+ = -f, \qquad B_+ = f^{-1}, \qquad C_+ = r_+^2, \qquad f := 1 + \frac{2|M|}{r_+},$$
$$\epsilon_\pm = 1, \tag{47}$$

where M is a negative constant.

In $\mathcal{M}^-$, the fastest outgoing null geodesic emanating from the center $(t_-, r_-) = (0, 0)$ makes the Cauchy surface, and it is the same equation in the previous example: $t_- = z_{ch} r_-$. z_{ch} is the smallest solution to Eq. (31). Also, other quantities relevant to our calculation are the same.

In $\mathcal{M}^+$, the outgoing null geodesic is given by

$$\frac{\mathrm{d}t_+}{\mathrm{d}r_+} = \frac{r_+}{r_+ + 2|M|}. \tag{48}$$

Especially, the null emitted from the center is explicitly given by integrating Eq. (48):

$$t_+ = r_+ - 2|M| \ln\left(\frac{r_+}{2|M|} + 1\right). \tag{49}$$

The condition for the both metrics to be same at Σ, Eq. (5), takes the form $R_-|_\Sigma = r_+|_\Sigma$, i.e.,

$$(1 - a z_{ch})^{2/3} r_-(\lambda)|_\Sigma = r_+(\lambda)|_\Sigma. \tag{50}$$

The parametric equation in $\mathcal{M}^+$ is

$$t_+ = r_+(\lambda) - 2|M| \ln\left(\frac{r_+(\lambda)}{2|M|} + 1\right), \qquad r_+ = r_+(\lambda),$$
$$\theta = \theta, \qquad \varphi = \varphi. \tag{51}$$

Basis vectors on Σ are

$$k_+^\alpha \partial_\alpha = \overset{\circ}{r}_+ f^{-1} \partial_t + \overset{\circ}{r}_+ \partial_r, \qquad N_\alpha^+ \mathrm{d}x^\alpha = -\frac{f}{2\overset{\circ}{r}_+}\mathrm{d}t_+ - \frac{1}{2\overset{\circ}{r}_+}\mathrm{d}r_+,$$
$$e_{(\theta)}^\alpha \partial_\alpha = \partial_\theta, \qquad e_{(\varphi)}^\alpha \partial_\alpha = \partial_\varphi. \tag{52}$$

Transverse curvature C_{lm}^+ is calculated as

$$C_{\lambda\lambda}^+ = 0, \qquad C_{ab}^+ = -\frac{f}{2 r_+ \overset{\circ}{r}_+} \sigma_{ab}^+, \tag{53}$$

where $\sigma_{ab}^+ \mathrm{d}x^a \mathrm{d}x^b := r_+^2 (\mathrm{d}\theta^2 + \sin^2\theta \mathrm{d}\varphi^2)$. Then, we have μ and p as

$$8\pi\mu = \frac{f}{r_+ \overset{\circ}{r}_+} - \frac{1}{z_{ch} R_\Sigma \overset{\circ}{r}_-}\left(\frac{2a}{3(1 - a z_{ch})^{1/3}} + 1\right), \tag{54}$$

$$8\pi p = \overset{\circ}{r}_- \frac{2a^2 z_{ch}}{9 r_- (1 - a z_{ch})^{4/3}}. \tag{55}$$

For calculation of $E_{\rm shell}$, the same as in the previous example, we adopt the 4-velocity of a comoving observer. Then, the final form for the shell energy is written by

$$E_{\rm shell} = \frac{z_{ch}|M|}{(1 - a z_{ch})^{2/3}} + \frac{R_\Sigma}{2}\left\{\frac{z_{ch}}{(1 - a z_{ch})^{2/3}} - \frac{2a}{3(1 - a z_{ch})^{1/3}} - 1\right\}. \tag{56}$$

In Eq. (56), the first term is constant, while the second term is linear in terms of R_Σ. Because the coefficient of the second term is positive [43], the energy increases monotonically as the null surface with R_Σ expands.

Comparing Eq. (56) with the previous case, Eq. (44), the first term on the right does not have R_Σ dependence. This term corresponds to the energy distribution of the negative mass Schwarzschild solution that is pointlike. Note here that in this example the null shell carries energy of the collapsing dust matter as well as energy relevant to the remnant negative mass.

In the next subsection, Sec. III C, we discuss the appearance of a negative-mass Schwarzschild solution (naked singularity) from a Minkowski spacetime by spontaneous emission of radiation. We can recover this case in the $a \to 0$ limit of Eq. (56). In this limit, we have $z_{ch} \to 1$, from Eq. (31), and $E_{\rm shell} \to |M|$.

The numerical plot of typical parameters for $E_{\rm shell}$ in Eq. (56) is shown in Fig. 3.

In Fig. 3, the energy of the shell is plotted for different values of initial density parameters. The mass of the negative of the Schwarzschild solution can be arbitrary. The first curve ($a = 0$) corresponds to Minkowski spacetime matching to a negative-mass Schwarzschild solution. As expected, the energy carried by the shell is equal to $|M|$.

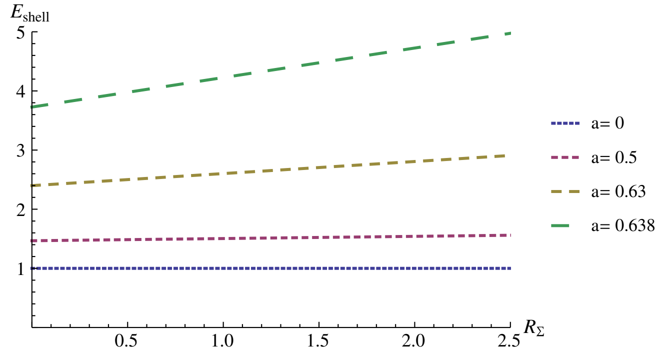

FIG. 3. Values of $E_{\rm shell}$ in Eq. (56) for each a. We fixed M, say, $|M| = 1$.

The subsequent curves have additional energy corresponding to the LTB of the collapsing dust.

The situation in this example is similar to the previous example, but the future of Σ is replaced with the negative-mass Schwarzschild solution. By operating junction conditions, we get Eq. (56) for the energy of the expanding null shell. As in the previous example, the shell's whole energy is a monotonically increasing function of R, and it diverges at infinity. At the same time the singularity forms, the null shell expands outward as the previous case does. However, the remnant singularity is much more serious than that of previous example due to the negative gravitational mass. Instant singularity, a special case mentioned earlier, can also be recovered in this example by taking the parameter $M = 0$.

C. Spontaneous decay of Minkowski, the end of inflation, and black hole formation

We consider several scenarios that denote the spontaneous decay of Minkowski, the end of inflation, and black hole formation. We can describe all of such scenarios under Schwarzschild–(anti-)de Sitter (AdS) solution in both spacetimes:

$$A_\pm = -f_\pm, \qquad B_\pm = f_\pm^{-1}, \qquad C_\pm = r_\pm^2,$$
$$f_\pm := 1 - \frac{2m_\pm}{r_\pm} - \frac{\Lambda_\pm}{3} r_\pm^2, \qquad \epsilon_+ = \epsilon_- =: \epsilon. \tag{57}$$

The condition that the two metrics are same on null hypersurface, Eq. (5), now yields just a simple relation,

$$r_+(\lambda)|_\Sigma = r_-(\lambda)|_\Sigma, \tag{58}$$

and consequently $\overset{\circ}{r}_+ = \overset{\circ}{r}_-$. $k_\pm^\alpha$ and $N_\alpha^\pm$ are given by

$$k_\pm^\alpha \partial_{\alpha\pm} = \epsilon_\pm \overset{\circ}{r}_\pm f_\pm^{-1} \partial_t^\pm + \overset{\circ}{r}_\pm \partial_r^\pm, \tag{59}$$

$$N_\alpha^\pm \mathrm{d}x^\alpha = -\frac{\epsilon_\pm f_\pm}{2\overset{\circ}{r}_\pm}\mathrm{d}t - \frac{1}{2\overset{\circ}{r}_\pm}\mathrm{d}r. \tag{60}$$

Transverse curvature on the both sides is now given by

$$C_{\lambda\lambda}^\pm = 0 \quad \text{and} \quad C_{ab}^\pm = -\frac{f_\pm \sigma_{ab}^\pm}{2r_\pm \overset{\circ}{r}_\pm}. \tag{61}$$

μ and p are written as

$$8\pi\mu = \frac{1}{r\overset{\circ}{r}}\left\{\frac{2}{r}(m_- - m_+) + \frac{r^2}{3}(\Lambda_- - \Lambda_+)\right\}, \tag{62}$$

$$p = 0, \tag{63}$$

where we defined $r := r_+(\lambda)|_\Sigma = r_-(\lambda)|_\Sigma$. When one adopts an observer who sticks in the coordinates in $\mathcal{M}^-$, a 4-velocity takes the form $u_-^\alpha \partial_\alpha = \partial_t$, and hence $E_{\rm shell}$ can be evaluated as

$$E_{\rm shell} = \epsilon\left\{(m_- - m_+) + \frac{r^3}{6}(\Lambda_- - \Lambda_+)\right\}. \tag{64}$$

Equation (64) describes the general result of shell energy seen by a distant observer. We find Eq. (64) is a quartic function of r. If the gap of the cosmological constant is zero, $[\Lambda] = 0$, the distant observer will measure a constant energy (luminosity). Otherwise, the energy is a function of r^3 that diverges at infinity.

Below, we investigate the models of a spontaneous decay of Minkowski, the end of inflation, and black hole formation as a consequence of contraction/expansion of the null shell. We consider these scenarios as special cases of Eq. (64).

1. Spontaneous decay of Minkowski

We consider a case of the Minkowski solution in $\mathcal{M}^-$ and the negative-mass Schwarzschild solution in $\mathcal{M}^+$. Then, we take parameters as follows:

$$m_- = 0, \qquad m_+ = -|m_+|, \qquad \Lambda_\pm = 0, \qquad \epsilon = +1. \tag{65}$$

This choice of geometries describes a spontaneous decay of Minkowski, a sudden appearance of a naked singularity that has a negative mass. In this case, the null energy emitted from the singularity is evaluated as

$$\mu = \frac{|m_+|}{4\pi r^2 \overset{\circ}{r}}, \qquad E_{\rm shell} = |m_+|. \tag{66}$$

Since a negative-mass Schwarzschild spacetime describes a naked singularity, an appearance of a naked singularity occurs in a flat spacetime after a null explosion having a positive energy.

One can consider another spontaneous decay model that shows more violent behavior than the previous one.

Suppose that the null shell starts to expand from the center in Minkowski spacetime, and also suppose that the inside of the null shell is AdS spacetime. Then, this is the situation that also describes a spontaneous decay of Minkowski, the instability of Minkowski spacetime. In this scenario, the past of Σ, i.e., $\mathcal{M}^-$, is Minkowski, and the future of Σ, i.e., $\mathcal{M}^+$, is AdS spacetime:

$$m_\pm = 0, \qquad \Lambda_- = 0, \qquad \Lambda_+ = -|\Lambda|, \qquad \epsilon = +1. \tag{67}$$

Then, we have

$$\mu = \frac{|\Lambda| r}{24\pi \overset{\circ}{r}}, \qquad E_{\rm shell} = \frac{|\Lambda|}{6} r^3, \tag{68}$$

which is a monotonically increasing function of r.

2. End of inflation

Let us take the Minkowski solution in $\mathcal{M}^-$ and the de Sitter solution in $\mathcal{M}^+$. This case is an example of the end of inflation and realized by taking parameters as follows:

$$m_\pm = 0, \qquad \Lambda_+ = 0, \qquad \Lambda_- > 0, \qquad \epsilon = +1. \tag{69}$$

Then, the energy is given by

$$\mu = \frac{\Lambda_- r}{24\pi \overset{\circ}{r}}, \qquad E_{\rm shell} = \frac{\Lambda_-}{6} r^3. \tag{70}$$

Another example of the end of inflation is given by taking the parameters as

$$m_\pm = 0, \qquad \Lambda_- > \Lambda_+, \qquad \epsilon = +1. \tag{71}$$

Then, the energy is given by

$$\mu = \frac{(\Lambda_- - \Lambda_+) r}{24\pi \overset{\circ}{r}}, \qquad E_{\rm shell} = \frac{(\Lambda_- - \Lambda_+)}{6} r^3. \tag{72}$$

3. Black hole formation

An imploding null shell can result in black hole formation. We take such an example by considering the choice of the Minkowski solution in $\mathcal{M}^-$ and positive-mass Schwarzschild solution in $\mathcal{M}^+$, *i.e.*,

$$m_- = 0, \qquad m_+ > 0, \qquad \Lambda_\pm = 0, \qquad \epsilon = -1. \tag{73}$$

Then, the energy is given by

$$\mu = \frac{m_+}{4\pi r^2 (-\overset{\circ}{r})}, \qquad E_{\rm shell} = m_+, \tag{74}$$

which is positive definite. Here, μ is positive because of shrink of the shell, i.e., $\overset{\circ}{r} < 0$.

4. Bubble nucleation

One can consider the phenomenological model of nucleation of the bubble, which is caused by transition of the false vacuum. Let us take parameters as follows:

$$m_\pm = 0, \qquad \Lambda_- > \Lambda_+, \qquad \epsilon = +1. \tag{75}$$

Then, the energy is given by

$$\mu = \frac{(\Lambda_- - \Lambda_+) r}{24\pi \overset{\circ}{r}}, \qquad E_{\rm shell} = \frac{(\Lambda_- - \Lambda_+)}{6} r^3. \tag{76}$$

In our case, the bubble propagates as the speed of light. The spacetime before the shell passes is de Sitter, and the spacetime after passing through the shell can be de Sitter ($\Lambda_+ > 0$), Minkowski ($\Lambda_+ = 0$), and AdS ($\Lambda_- < 0$).

IV. CONCLUSION

We developed models of a radiation emitted from regions with extremely high curvature. For this purpose, we derived a general formula that describes an imploding or exploding null shell in general spherically symmetric spacetime. The energy is defined and evaluated as a surface energy of a null hypersurface, the null shell.

In general relativity, since one does not have predictability on the evolution of a spacetime after a Cauchy horizon is formed, the future of spacetimes made by matching on Cauchy horizons is not a unique specification. Thus, we have investigated examples of filling the spacetime inside of the Cauchy horizon and showed possibilities on the future evolution of a singularity formation. We have proposed several models that can describe dynamical processes of radiating energy, followed by the gravitational collapse of a star.

In the first example, we constructed a model of energy emission by matching two self-similar marginally bound LTB spacetimes at their Cauchy horizons. Since the equation of the Cauchy horizon in the self-similar dust is well known, we can operate the explicit calculation for the matching. Our model describes an isotropic energy emission from the singularity. Because of the construction of this model, a null shell starts expanding from the position of the singularity and carries certain energy that propagates along the Cauchy horizon. If we assume positive definiteness of the propagating energy, a condition $a_- > a_+$ must hold. We also derived an equation for the surface pressure that is defined on Σ. We found the surface energy μ is caused by the difference between the initial profiles κ_+ and κ_- in the two dust spacetimes. Such a structure is qualitatively the same as a model presented by Jhingan *et al.* [44]. They analyzed a model of matching the two Vaidya spacetimes at their Cauchy horizons and found the surface energy is obtained as the difference between the mass function in the (+) side and in the (−) side.

We also proposed various examples focused on static spherically symmetric models. In most examples, $E_{\rm shell}$, or equivalently the absolute value of luminosity, is proportional to the power of r. It is clear from Eq. (64) that luminosity is constant if and only if the both cosmological constants are identical. Thus, the increasing property of luminosity in Eqs. (68), (70), (72), and (76) is caused by the presence of difference between Λ_+ and Λ_-. Since the cosmological constant can be interpreted as cosmological fluid, such an increasing shell's energy should be supplied by the fluid, which is similar to the previous example treating dust spacetime in which increasing luminosity is caused by infalling dust fluid.

Constant energy or luminosity, such as in the case of spontaneous decay of Minkowski, occurs only if $\Lambda_+ = \Lambda_-$. Since there is no energy supply, constant energy is taken to be the pure energy emitted from the central singularity.

We stress that the origin of emitted energy $E_{\rm shell}$ is divided into two parts: energy itself from singularity and energy supply from the fluid around the shell. Expanding null shell must increase its energy by absorbing the energy of the neighboring fluid. In some parts of the paper, we investigated the behavior of expanding null shells in spacetime filled with fluid (self-similar LTB or cosmological fluid). In such situations, dust/cosmological fluid spreads to spatial infinity as a simple example in calculation. In this case, due to the constant energy supply to the shell from the fluid, a distant observer would measure a violently energetic and luminous shell. On the other hand, the shell propagates having constant energy/luminosity in the case without fluid.

Lastly, we note that in the astrophysical situation a fluid spreads to a certain radius, so the energy supply is cut off at the radius, and after the null shell passes through that radius, the shell's energy/luminosity should become a constant. Thus, such energy emission models created from higher curvature regions could be one of the possible candidates playing the role of high-energy phenomena in the Universe.

ACKNOWLEDGMENTS

T. K. thanks Ken-ichi Nakao for stimulating discussions. The authors wish to thank Vitor Cardoso, Chul-Moon Yoo, and Taishi Ikeda for valuable comments and discussions. This work was partially supported by JSPS KAKENHI Grant No. JP26400282 (T. H.). S. J. thanks I. H. Dwivedi for discussions.

[1] B. P. Abott *et al.* (LIGO Scientific Collaboration and Virgo Collaboration), Phys. Rev. Lett. **116**, 061102 (2016).
[2] B. P. Abott *et al.* (LIGO Scientific and Virgo Collaborations), Phys. Rev. Lett. **116**, 241103 (2016).
[3] B. P. Abott *et al.* (LIGO Scientific and Virgo Collaborations), Phys. Rev. Lett. **118**, 221101 (2017).
[4] B. P. Abott *et al.* (LIGO Scientific and Virgo Collaborations), Phys. Rev. Lett. **119**, 141101 (2017).
[5] B. P. Abott *et al.* (LIGO Scientific and Virgo Collaborations), Phys. Rev. Lett. **119**, 161101 (2017).
[6] W. D. Apel *et al.* (LIGO Scientific and Virgo Collaborations), Astrophys. J. Lett. **848**, 1 (2017).
[7] R. Penrose, Phys. Rev. Lett. **14**, 57 (1965).
[8] S. W. Hawking, Proc. R. Soc. A **300**, 187 (1967).
[9] R. Geroch and G. T. Horowitz, *General Relativity: An Einstein Centenary Survey*, edited by S. W. Hawking and W. Israel (Cambridge University Press, Cambridge, England, 1979); J. M. M. Senovilla, Gen. Relativ. Gravit. **29**, 701 (1997).
[10] R. Penrose, Riv. Nuovo Cimento Soc. Ital. Fis. **1**, 252 (1969); Gen. Relativ. Gravit. **34**, 1141 (2002).
[11] J. R. Oppenheimer and H. Snyder, Phys. Rev. **56**, 455 (1939).
[12] D. M. Eardley and L. Smarr, Phys. Rev. D **19**, 2239 (1979).
[13] M. D. Roberts, Gen. Relativ. Gravit. **21**, 907 (1989).
[14] A. Ori and T. Piran, Phys. Rev. Lett. **59**, 2137 (1987).
[15] D. Christodoulou, Commun. Math. Phys. **93**, 171 (1984).
[16] P. S. Joshi and I. H. Dwivedi, Phys. Rev. D **47**, 5357 (1993).
[17] T. Harada, Phys. Rev. D **58**, 104015 (1998).
[18] T. Harada and H. Maeda, Phys. Rev. D **63**, 084022 (2001).
[19] F. I. Cooperstock, S. Jhingan, P. S. Joshi, and T. P. Singh, Classical Quantum Gravity **14**, 2195 (1997).
[20] S. S. Deshingkar, S. Jhingan, and P. S. Joshi, Gen. Relativ. Gravit. **30**, 1477 (1998); S. M. C. V. Goncalves and S. Jhingan, Int. J. Mod. Phys. D **11**, 1469 (2002).
[21] S. K. Chakrabarti and P. S. Joshi, Int. J. Mod. Phys. D **03**, 647 (1994).
[22] T. P. Singh, Gen. Relativ. Gravit. **30**, 1563 (1998).
[23] W. A. Hiscock, L. G. Williams, and D. M. Eardley, Phys. Rev. D **26**, 751 (1982).
[24] C. Vaz and L. Witten, Phys. Lett. B **325**, 27 (1994).
[25] C. Vaz and L. Witten, Classical Quantum Gravity **12**, 2607 (1995).
[26] C. Vaz and L. Witten, Classical Quantum Gravity **13**, L59 (1996).
[27] S. Barve, T. P. Singh, C. Vaz, and L. Witten, Nucl. Phys. **B532**, 361 (1998).
[28] S. Barve, T. P. Singh, C. Vaz, and L. Witten, Phys. Rev. D **58**, 104018 (1998).
[29] C. Vaz and L. Witten, Phys. Lett. B **442**, 90 (1998).
[30] T. Harada, H. Iguchi, and K. i. Nakao, Phys. Rev. D **61**, 101502 (2000).
[31] T. Harada, H. Iguchi, and K. i. Nakao, Phys. Rev. D **62**, 084037 (2000).

[32] T. Harada, H. Iguchi, K. i. Nakao, T. P. Singh, T. Tanaka, and C. Vaz, Phys. Rev. D **64**, 041501 (2001).
[33] H. Iguchi and T. Harada, Classical Quantum Gravity **18**, 3681 (2001).
[34] T. Harada, H. Iguchi, and K. i. Nakao, Prog. Theor. Phys. **107**, 449 (2002).
[35] H. Iguchi, K. i. Nakao, and T. Harada, Phys. Rev. D **57**, 7262 (1998).
[36] H. Iguchi, T. Harada, and K. i. Nakao, Prog. Theor. Phys. **101**, 1235 (1999).
[37] H. Iguchi, T. Harada, and K. i. Nakao, Prog. Theor. Phys. **103**, 53 (2000).
[38] C. Barrabés and P. A. Hogan, *Singular Null Hypersurface in General Relativity* (World Scientific, Singapore, 2003), Chap. 5.
[39] E. Poisson, *A Relativist's Toolkit* (Cambridge University Press, Cambridge, England, 2007), Chap. 3; E. Poisson, arXiv:gr-qc/0207101.
[40] B. J. Carr and A. A. Coley, Gen. Relativ. Gravit. **37**, 2165 (2005).
[41] S. Barve, T. P. Singh, C. Vaz, and L. Witten, Classical Quantum Gravity **16**, 1727 (1999).
[42] E. M. Duffy and B. C. Nolan, arXiv:1108.1103.
[43] From Eq. (29) and Eq. (30), we have $z=\frac{1-\frac{az}{3}}{(1-az)^{1/3}}$. $(1-az)^{-1/3}\geq 1$ holds because of $0\leq az<1$. For $X\geq 1$, one gets the inequality $X^{-1/3}\geq X^{-1}$. Thus, we get the inequality for z:

$$z=\frac{1-\frac{az}{3}}{(1-az)^{1/3}}\geq\frac{1-\frac{az}{3}}{1-az}\geq 1.$$

On the other hand, if the coefficient of the second term in Eq. (56) can be negative; then, by recasting the coefficient with using the relation in above equation, the condition for the negativity can be simply written as $z^3<1-a^2z^2/9$, i.e., $z<1$. However, according to above equation, we have $z\geq 1$. This proves the non-negativity for the coefficient of the second term in Eq. (56).
[44] S. Jhingan, I. H. Dwivedi, and S. Barve, Phys. Rev. D **84**, 024001 (2011).